MicroRNA-150 regulates the cytotoxicity of natural killers by targeting perforin-1

Nayoung Kim, PhD,[a] Miju Kim, PhD,[c,d] Sohyun Yun, PhD,[a] Junsang Doh, PhD,[c,d] Philip D. Greenberg, MD,[e] Tae-Don Kim, PhD,[a,b] and Inpyo Choi, PhD[a,b] *Daejeon and Pohang, Korea, and Seattle, Wash*

Background: Perforin-1 (Prf1) is the predominant cytolytic protein secreted by natural killer (NK) cells. For a rapid immune response, resting NK cells contain high Prf1 mRNA concentrations while exhibiting minimal cytotoxicity caused by a blockage of Prf1 protein synthesis, implying that an unknown posttranscriptional regulatory mechanism exists.
Objective: We sought to determine whether microRNA-150 (miR-150) posttranscriptionally regulates Prf1 translation in both mouse and human NK cells at rest and at various time points after activation.
Methods: Mouse NK cells with a targeted deletion of miR-150 (miR-150$^{-/-}$ NK cells), primary human NK cells, and NK92 MI cells were used to investigate the role of miR-150 in NK cells. NK cell cytotoxicity assays and Western blotting proved that activated miR-150$^{-/-}$ NK cells expressed upregulated Prf1, augmenting NK cell cytotoxicity. When immunodeficient mice were injected with miR-150$^{-/-}$ NK cells, there was a significant reduction in tumor growth and metastasis of B16F10 melanoma.
Results: We report that miR-150 binds to 3′ untranslated regions of mouse and human Prf1, posttranscriptionally downregulating its expression. Mouse wild-type NK cells displayed downregulated miR-150 expression in response to IL-15, which led to corresponding repression and induction of Prf1 during rest and after IL-15 activation, respectively.
Conclusion: Our results indicate that miR-150 is a common posttranscriptional regulator for Prf1 in mouse and human NK cells that represses NK cell lytic activity. Thus the therapeutic control of miR-150 in NK cells could enhance NK cell–based immunotherapy against cancer, providing a better clinical outcome. (J Allergy Clin Immunol 2014;134:195-203.)

Key words: *miR-150, NK cells, perforin-1, NK cell cytotoxicity, post-transcriptional regulation, immunotherapy, tumor growth and metastasis*

Natural killer (NK) cells kill target cells predominantly by secreting granule toxins, including perforin-1 (Prf1) and granzymes.[1-3] Prf1 is a pore-forming protein, and granzymes are structurally related serine proteases that lyse target cell protein at specific aspartate residues.[4,5] Prf1 disturbs the target cell membrane and facilitates the entry, trafficking, or both of granzymes.[6] Unlike multiple granzymes, which can compensate each other, Prf1 is encoded by a single gene and does not have any functional redundancy.[7]

NK cells kill target cells "naturally" without prior antigen-specific recognition, allowing for rapid induction of lytic activity.[8] For prompt immune responses, resting NK cells are in a "prearmed" state, containing high concentrations of Prf1 mRNA, but they are minimally cytotoxic because of a blockage of Prf1 translation.[9] On target recognition, activated NK cells immediately arm themselves with preformed Prf1 mRNA, correlating with an increase in Prf1 protein levels. Therefore Prf1 is posttranscriptionally regulated by unknown regulators in resting NK cells.

MicroRNAs (miRNAs) are small noncoding RNAs of approximately 22 nucleotides that function as posttranscriptional inhibitors complementary to the 3′ untranslated region (UTR) of their target mRNAs.[10] Over the past few years, emerging data have implied that endogenously generated miRNAs are posttranscriptional regulators of immune cell development and function.[11] miR-150 has been identified as a lymphocyte-specific miRNA because it is predominantly expressed in the lymph nodes, spleen, and thymus and is highly upregulated during lymphocyte maturation. miR-150 expression increases sharply in mature B and T lymphocytes, as well as in mature NK and invariant NK T cells, although not in their progenitors.[12-16]

Although miR-150 expression is upregulated during lymphocyte maturation, it is downregulated again during the activation of mature B and T cells. Xiao et al[14] reported that miR-150 expression was downregulated in activated B cells and that miR-150–deficient mice exhibit enhanced humoral and T cell–dependent antibody responses with increased steady-state immunoglobulin levels. Collectively, miR-150 appears to be inversely associated

From [a]the Immunotherapy Research Center, Korea Research Institute of Bioscience and Biotechnology (KRIBB), Daejeon; [b]the Department of Functional Genomics, University of Science and Technology (UST), KRIBB, Daejeon; [c]the School of Interdisciplinary Bioscience and Bioengineering (I-Bio) and [d]the Department of Mechanical Engineering, POSTECH, Pohang; and [e]the Departments of Immunology and Medicine, University of Washington School of Medicine, and Fred Hutchinson Cancer Research Center, Seattle.

Supported in part by grants from the GRL project (FGM1401223); the Ministry of Education, Science & Technology; the Korean Health Technology R&D Project (A121934); the Ministry of Health and Welfare; the KRIBB Research Initiative Program; and the Basic Science Research Program through the National Research Foundation of Korea (RBM0261312). P.D.G. was supported in part by grants from the KRIBB Research Initiative Program and the National Institutes of Health (CA33084).

Disclosure of potential conflict of interest: I. Choi's institution has received grants from the GRL project, the Heath Technology R&D Project, the KRIBB Research Initiative Program, and the Basic Science Research Program. P. D. Greenberg's institution received a grant from the National Cancer Institute; he has been compensated by Innate Pharma for board membership, as well as for consultant services; and he has received stock/stock options from Innate Pharma. The rest of the authors declare that they have no relevant conflicts of interest.

Received for publication September 6, 2013; revised January 15, 2014; accepted for publication February 14, 2014.

Available online March 31, 2014.

Corresponding author: Inpyo Choi, PhD, Immunotherapy Research Center, Korea Research Institute of Bioscience and Biotechnology, 125 Gwahak-ro, Yuseong, Daejeon 305-806, Republic of Korea. E-mail: ipchoi@kribb.re.kr. Or: Tae-Don Kim, PhD, Immunotherapy Research Center, Korea Research Institute of Bioscience and Biotechnology, 125 Gwahak-ro, Yuseong, Daejeon 305-806, Republic of Korea. E-mail: tdkim@kribb.re.kr.

0091-6749

http://dx.doi.org/10.1016/j.jaci.2014.02.018

Abbreviations used
AANAT: Aralkylamine N-acetyltransferase
DMEM: Dulbecco modified Eagle medium
E/T: Effector/target
GAPDH: Glyceraldehyde-3-phosphate dehydrogenase
GzmB: Granzyme B
HEK: Human embryonic kidney
miRNA: MicroRNA
NeoR: Neomycin resistance gene
NK: Natural killer
PI: Propidium iodide
Prf1: Perforin-1
UTR: Untranslated region
WT: Wild-type

with the immunologic functions of activated B and T cells, but a relationship between miR-150 and the activation of NK cells has not yet been shown.

In this study we report that miR-150 binds to the 3′ UTR of mouse and human Prf1, posttranscriptionally downregulating its expression. Mouse wild-type (WT) NK cells exhibited biphasic upregulated and downregulated miR-150 expression in response to IL-15, which led to corresponding repression and induction of Prf1 during rest and after IL-15 activation, respectively. Primary human NK cells also display downregulated miR-150 and augmented Prf1 in response to IL-15. Our results suggest that miR-150$^{-/-}$ NK cells might provide clinical benefit to minimize spontaneous activation in resting NK cells while maximizing cytotoxicity in activated NK cells. Therapeutic modulation of miR-150 might be a promising new approach for enhancing NK cell–mediated immunotherapy to treat various human pathologies.

METHODS

For a detailed description of the methods used in this study, see Tables E1 and E2 and the Methods section in this article's Online Repository at www.jacionline.org.

RESULTS

miR-150 expression is inversely proportional to Prf1 protein expression in both mouse and human NK cells during IL-15 activation

The expression of miR-150 in mouse WT NK cells exhibited a biphasic pattern during IL-15 stimulation. The miR-150 level was sharply increased nearly 2-fold at 4 hours and maintained for a time. Then its level was markedly decreased to less than the level of resting NK cells at 24 hours and further downregulated at 72 hours. The miR-150 level was negatively associated with expression of Prf1 protein (Fig 1, *A*). Primary human NK cells showed gradually decreased expression of miR-150 and increased levels of Prf1 protein in response to IL-15 (Fig 1, *B*). In both mouse and human NK cells, relatively high abundance of miR-150 and sustained expression of Prf1 and granzyme B (GzmB) protein were observed during the first 6 hours of IL-15 stimulation. Then Prf1 and GzmB protein expression started to increase, accompanied by reduced expression of miR-150 at 24 hours (Fig 1, *C* and *D*, top). In addition, GzmB mRNA expression was notably increased in a time-dependent manner correlating with an increase in GzmB protein levels, but abundant mRNA of Prf1 in resting NK cells remained largely unchanged during IL-15 activation in both mouse and human NK cells (Fig 1, *C* and *D*, bottom). This implies that Prf1 could be posttranscriptionally repressed by miR-150 in NK cells at rest and earlier time points after IL-15 activation.

miR-150$^{-/-}$ NK cells have augmented Prf1 protein expression and enhanced NK cell cytotoxicity

Resting WT and miR-150$^{-/-}$ NK cells minimally expressed Prf1 protein, but Prf1 protein was amplified in miR-150$^{-/-}$ NK cells at 48 and 72 hours of IL-15 stimulation. However, Prf1 mRNA abundance did not change over time (Fig 2, *A*). After 48 hours of IL-15 stimulation, miR-150$^{-/-}$ NK cells exhibited enhanced cytotoxicity by approximately 2-fold at an effector/target (E/T) ratio of 5:1 (Fig 2, *B*). Collectively, abundant Prf1 mRNA was posttranscriptionally suppressed in resting NK cells, but miR-150$^{-/-}$ NK cells augmented Prf1 protein expression and cytotoxicity on IL-15 activation.

WT and miR-150$^{-/-}$ NK cells have similar NK cell receptor profiles, degranulation, and death receptor/ligand interactions

NK cells express various receptors to recognize target cells. Therefore we examined a broad range of activating NK cell receptors (NKG2D, NKp46, and Ly49D), inhibitory receptors (Ly49C/I, Ly49G2, and Ly49A), IL-15 receptors (CD122 and CD132), and chemokine receptors (CXCR5 and CCR6). IL-15–activated WT and miR-150$^{-/-}$ NK cells displayed similar frequencies in the receptor repertoire, including IL-15 receptors, and little or no chemokine receptor expression (Fig 3, *A*). It led to similar NK cell degranulation evidenced by the intensity of CD107a in WT and miR-150$^{-/-}$ NK cells after treatment with antibody against NKp46 in the presence or absence of target cells (Fig 3, *B*). NK cell cytotoxicity can also be mediated in the absence of Prf1 through engagement of death receptors (eg, Fas/CD95) on target cells through their cognate ligands (eg, Fas ligand) on NK cells.[17] We investigated the levels of 2 key effector ligands, Fas ligand and TNF-related apoptosis-inducing ligand, and the death receptor CD95 in IL-15–activated NK cells. miR-150 had no profound effects on the expression of these ligands and receptors (Fig 3, *A* and *C*). These data suggest that the augmented cytotoxicity of miR-150$^{-/-}$ NK cells is caused predominantly by enhanced Prf1 and not by significant changes in NK cell receptor profiles, IL-15 receptor–mediated signaling pathways, or death receptor/ligand interactions.

miR-150$^{-/-}$ NK cells show that potent lytic granules hit at the immunologic synapse

NK cells are functionally heterogeneous, and thus only a small portion of NK cells kill target cells.[18] Lytic granules of NK cells were labeled with LysoSensor Green, and target cells were labeled with DDAO-SE and then cocultured in propidium iodide (PI)–containing media to assess the dynamics of individual NK cell cytotoxicity. Larger amounts of lytic granules containing Prf1 and GzmB were found in miR-150$^{-/-}$ NK cells

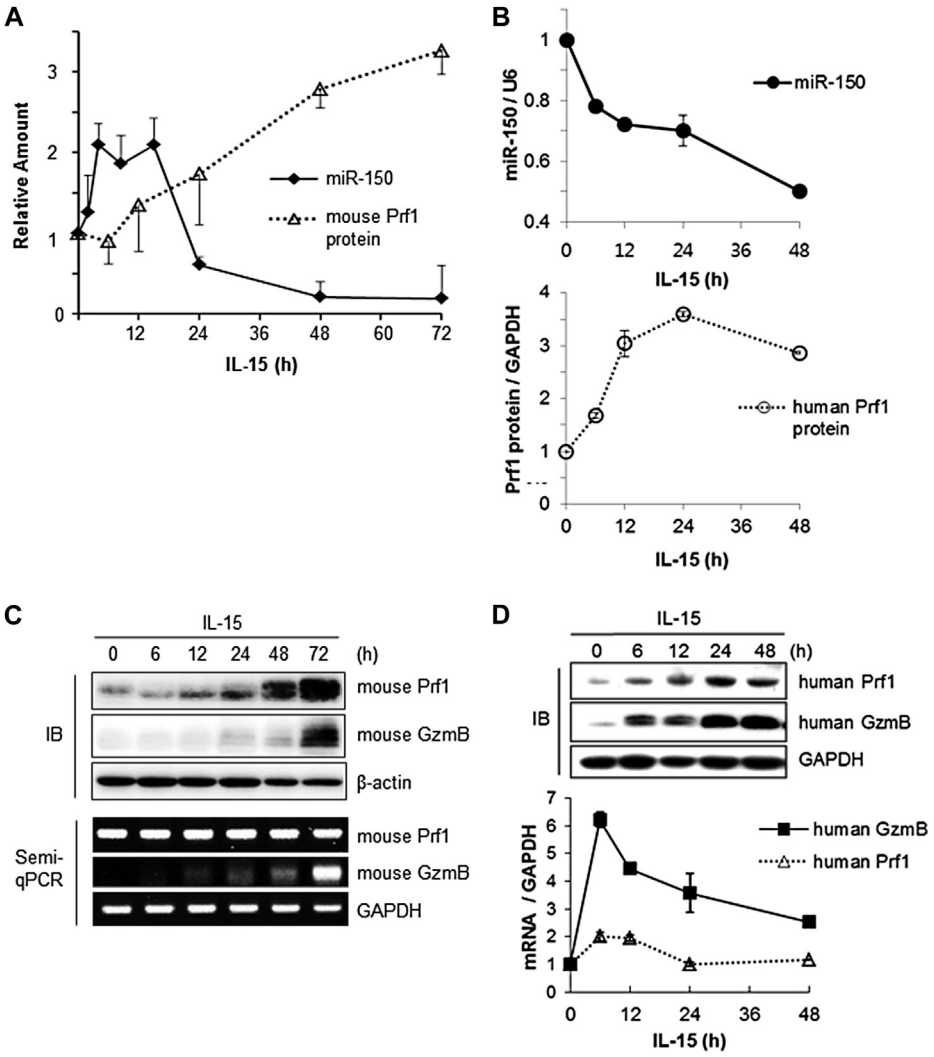

FIG 1. miR-150 is involved in the posttranscriptional regulation of Prf1 in NK cells. **A** and **B,** miR-150 and Prf1 protein levels were inversely plotted as means ± SDs in primary mouse (Fig 1, *A*) and human (Fig 1, *B*) NK cells. **C** and **D,** Protein and mRNA levels of Prf1 and GzmB were determined in mouse (Fig 1, *C*) and human (Fig 1, *D*) NK cells during IL-15 stimulation. Results are representative of 3 independent experiments.

than in WT NK cells, as indicated by microscopic granule intensity, showing an approximately 2-fold increase (Fig 4, *A*). In accordance, mean fluorescence intensity values of intracytoplasmic Prf1 determined by means of flow cytometry showed an increased Prf1 protein level in miR-150$^{-/-}$ NK cells (Fig 4, *B*). Additionally, WT and miR-150$^{-/-}$ NK cells were stained with CD107a, which is a sensitive marker of NK cell degranulation,[19] in the absence or presence of target cells. WT and miR-150$^{-/-}$ NK cells were minimally degranulated without targets but substantially degranulated after simulation with target cells. However, miR-150 had no significant effects on the extent of degranulation, and thus the overall degree of degranulation was similar in WT and miR-150$^{-/-}$ NK cells (Fig 4, *C*).

To understand NK cell–target cell interactions, we examined sequential stages of lytic synapses: the initiation, the effector, and termination stages. In the initiation stage NK cells transiently contact target cells with either diffused granules (step A) or polarized granules (step B). In the effector stage NK cells formed stable contacts with their targets and polarized lytic granules to distal poles (step C). Then lytic granules were transported to the immunologic synapse (step D). In the termination stage NK cells eventually killed target cells, as determined either by the formation of membrane blebs (step E) or an increase in PI fluorescence (Fig 4, *D*, right panel). These sequential steps are shown in Fig 4, *E*. Among NK cells encountering target cells, the percentages of NK cells remaining at each step at the end of 2-hour time-lapse imaging were measured and plotted in Fig 4, *F* (see Videos E1-E5 in this article's Online Repository at www.jacionline.org for each case). The kinetics of steps C, D, and E in WT and miR-150$^{-/-}$ NK cells were further assessed at various time points after coculture. Throughout the experiments, the higher percentage of WT NK cells remained at step D, but miR-150$^{-/-}$ NK cells exhibited higher cytotoxicity than WT NK cells when the duration of NK cell–target cell contact became longer than 60 minutes (Fig 4, *G* and *H*). This suggests that polarized granules in WT NK

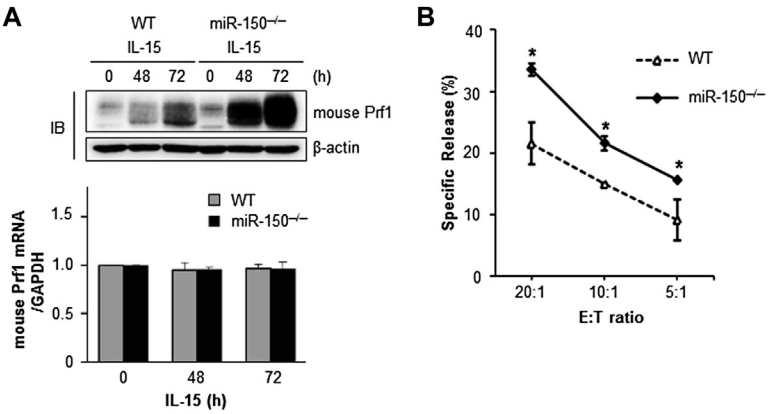

FIG 2. miR-150$^{-/-}$ NK cells exhibit upregulation of Prf1 and enhanced NK cell cytotoxicity. **A,** Protein and mRNA levels of Prf1 in WT and miR-150$^{-/-}$ NK cells after stimulation with IL-15. **B,** NK cell cytotoxicity was measured by using standard 4-hour ^{51}Cr-release assays. Data represent means ± SDs of 3 independent experiments. *$P < .05$, Student *t* test.

synapses might not be as effective as those in miR-150$^{-/-}$ NK cells to kill target cells. Because the levels of degranulation were comparable between WT and miR-150$^{-/-}$ NK cells (Fig 4, *C*), it is likely that miR-150$^{-/-}$ NK cells exhibit more potent lytic hits to target cells than WT NK cells, potentially because of higher content of lytic granules.

miR-150 directly targets Prf1 in both mouse and human NK cells

Aralkylamine N-acetyltransferase (AANAT) reporter assays were performed to test whether miR-150 directly targets Prf1.[20] AANAT reporter plasmids contain a neomycin resistance gene *(NeoR)* and AANAT coding region attached to GzmB 3′ UTR or Prf1 3′ UTR (Fig 5, *A*). According to the miRanda algorithm (www.microrna.org), miR-150 has 1 putative binding site in the 3′ UTR of mouse Prf1 (Fig 5, *B*). Moreover, it has a predicted binding site in the 3′ UTR of both human GzmB and Prf1, which have less complementary base pairing compared with mouse Prf1 (Fig 5, *B* and *C*). The miR-150 mimic did not change the expression of AANAT containing the 3′ UTR of mouse or human GzmB, suggesting GzmB was not the real target of miR-150. In contrast, miR-150 mimic significantly reduced the expression of AANAT containing mouse Prf1 3′ UTR in a dose-dependent manner (Fig 5, *D*, top) and human Prf1 3′ UTR to a lesser extent, as predicted by less complementarity (Fig 5, *E*, top). The miR-150 mutant, which had mutations in the 5′ end of miRNA (referred to as the seed region; Fig 5, *B* and *C*), lost binding capacity to the target and thus attenuated its inhibitory effects on mouse or human Prf1 3′ UTR (Fig 5, *D* and *E*, top). The levels of AANAT mRNA were normalized to those of NeoR mRNA to confirm that these phenomena dominantly occurred by miR-150–mediated AANAT reduction and were not caused by exogenous AANAT mRNA. Minimal AANAT mRNA changes were observed among transfected cells (Fig 5, *D* and *E*, bottom). AANAT mRNA levels were relatively higher in human Prf1 (>1.6-fold), but the AANAT protein expression was rather downregulated by the miR-150 mimic (Fig 5, *E*, bottom, lane 2). Taken together, these data suggest that Prf1 is a conserved functional target of miR-150 in both mouse and human NK cells.

Lentivirus-mediated overexpression of miR-150 shows a significant decrease in Prf1 levels and diminished NK cell–mediated cytotoxicity

miR-150$^{-/-}$ NK cells were transduced by lentivirus containing miR-150 precursor (LV-miR150) and cultured in a high concentration of IL-15 (100 ng/mL) for 2 days to test whether miR-150 overexpression and miR-150 deficiency would cause opposite effects on mouse or human NK cells. Lentivirus-mediated upregulation of miR-150 markedly repressed Prf1 protein expression compared with that seen in cells transduced with a control vector (Fig 6, *A*), which led to diminished NK cell cytotoxicity (Fig 6, *B*). In this case higher NK cell cytotoxicity was observed at a high concentration of IL-15 (100 ng/mL; Fig 6, *B*) compared with a modest concentration of IL-15 (25 ng/mL; Fig 2, *B*) at the same E/T ratio.

Compared with *in vitro*–differentiated human mature NK cells, NK92 MI cells expressed a significantly low level of endogenous miR-150 (Fig 6, *C*) and thus were selected for applying lentivirus-mediated overexpression. During lentiviral transduction, the miR-150 level in NK92 MI cells was increased in a time-dependent manner (Fig 6, *D*). Modest upregulation of miR-150 after 2 days of lentiviral transduction did not change human Prf1 protein, but robust expression of miR-150 significantly inhibited Prf1 production at 4 days after lentivirus 150 transduction (Fig 6, *D* and *E*), which contributed to reduced NK cell cytotoxicity (Fig 6, *F*). Collectively, these data imply that overexpression of miR-150 can act as a negative regulator of NK cell lytic activity by repressing Prf1 in both mouse and human NK cells.

miR-150$^{-/-}$ NK cells significantly reduce tumor growth and metastasis in immunocompromised mice

To investigate the role for miR-150 in immune surveillance against tumor cells *in vivo*, activated NK cells were injected intravenously, and then B16F10 melanoma were transplanted subcutaneously into Rag2$^{-/-}\gamma C^{-/-}$ mice, which lack B, T, and NK cells.[21] The adoptive transfer of miR-150$^{-/-}$ NK cells significantly reduced tumor volumes to an average of 71.23 ± 20.31 mm^3 (mean ± SD, n = 5), but WT NK cells less substantially

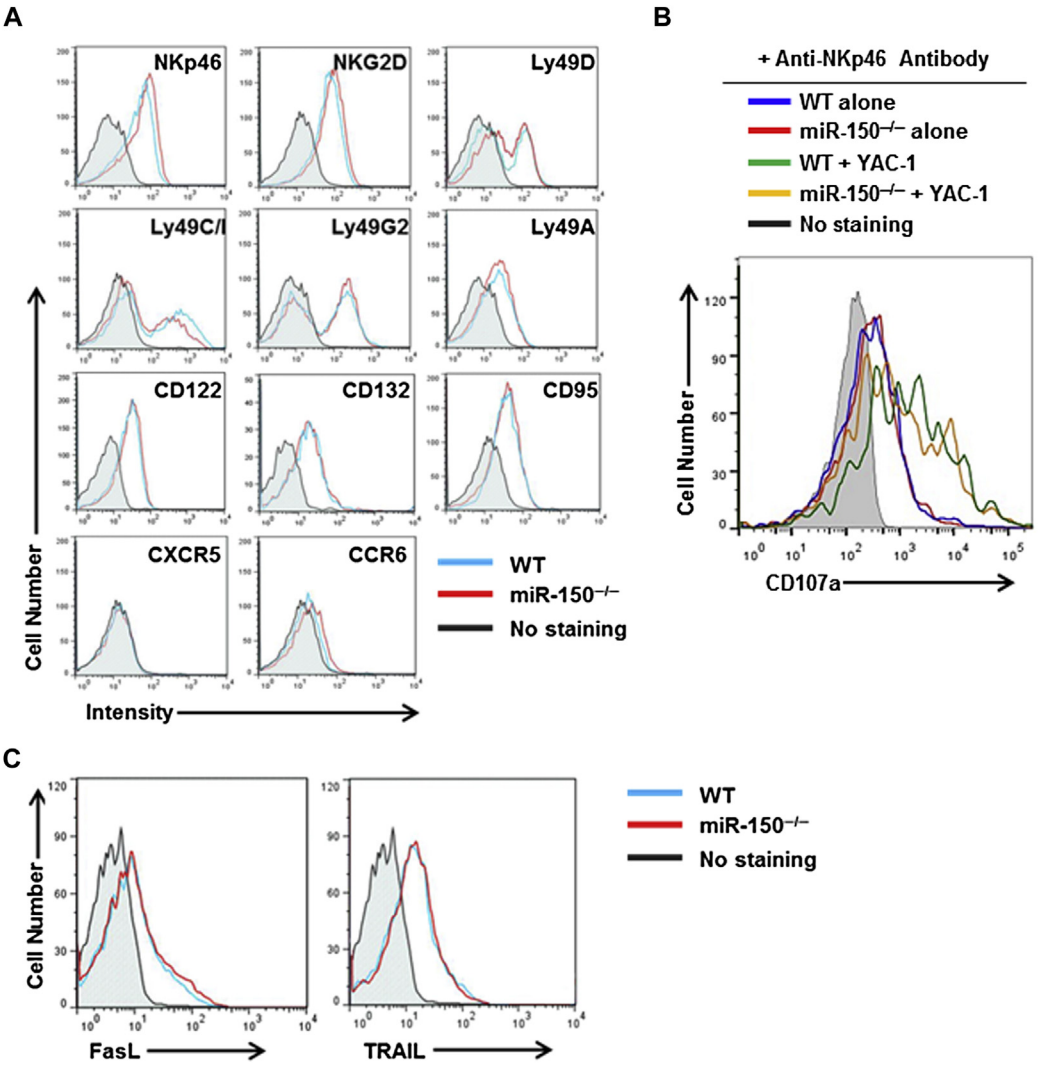

FIG 3. miR-150 has no significant effects on NK cell receptor profiles **(A)**, degranulation **(B)**, and death receptor/ligand interactions **(C)**. WT and miR-150$^{-/-}$ NK cells were cultured in IL-15 for 48 hours, and then cell surfaces were stained with indicated antibodies. Anti-NKp46 antibody was used to activate NKp46 receptors on NK cells. Data represent means ± SDs of 3 independent experiments. *FasL*, Fas ligand; *TRAIL*, TNF-related apoptosis-inducing ligand.

reduced tumor volumes, with an average of 146.62 ± 109.34 mm^3 (mean ± SD, n = 5) on day 11 after B16F10 implantation (Fig 7, *A*).

NK cells also play critical roles in reducing lung metastasis in various murine cancer models, and Prf1 is highly involved in the inhibition of tumor metastasis.[22] Activated WT and miR-150$^{-/-}$ NK cells were injected intravenously and then highly metastatic murine B16F10 cells were injected into the tail veins of Rag2$^{-/-}\gamma C^{-/-}$ mice at 2 days after NK cell transplantation to define the potential role for miR-150 in limiting lung metastasis of melanoma *in vivo*. The numbers of pulmonary metastatic colonies were quantitated and photographed at 14 days after B16F10 implantation (Fig 7, *B* and *C*). miR-150$^{-/-}$ NK cells effectively inhibited lung metastasis of B16F10 melanoma to an average of 170.71 ± 25.23 (mean ± SD, n = 7) compared with WT NK cells, with an average of 65.67 ± 21.42 (mean ± SD, n = 6; Fig 7, *B*). Taken together, these results demonstrate that miR-150$^{-/-}$ NK cells exhibit augmented NK cell cytotoxicity against tumor growth and lung metastasis of B16F10 melanoma in immunodeficient mice.

DISCUSSION

Prf1 was first isolated and characterized from cytotoxic lymphocytes in the mid-1980s, and significant progress has been made in understanding how NK cells use Prf1 to eliminate target cells. However, our knowledge of how preformed Prf1 mRNA is posttranscriptionally regulated in resting NK cells is still limited. Recent achievements have highlighted the importance of miRNA-mediated Prf1 regulation in human NK cells, and 2 studies have been summarized.[23,24] A study from our laboratory demonstrated that miR-27a* targeted the 3′ UTRs of Prf1 and GzmB in *in vitro*–differentiated human NK cells at rest or after IL-15 activation.[20] However, freshly isolated resting human NK cells expressed very low levels of miR-27a*.[25] This suggests that *in vitro*–differentiated human NK cells that result from

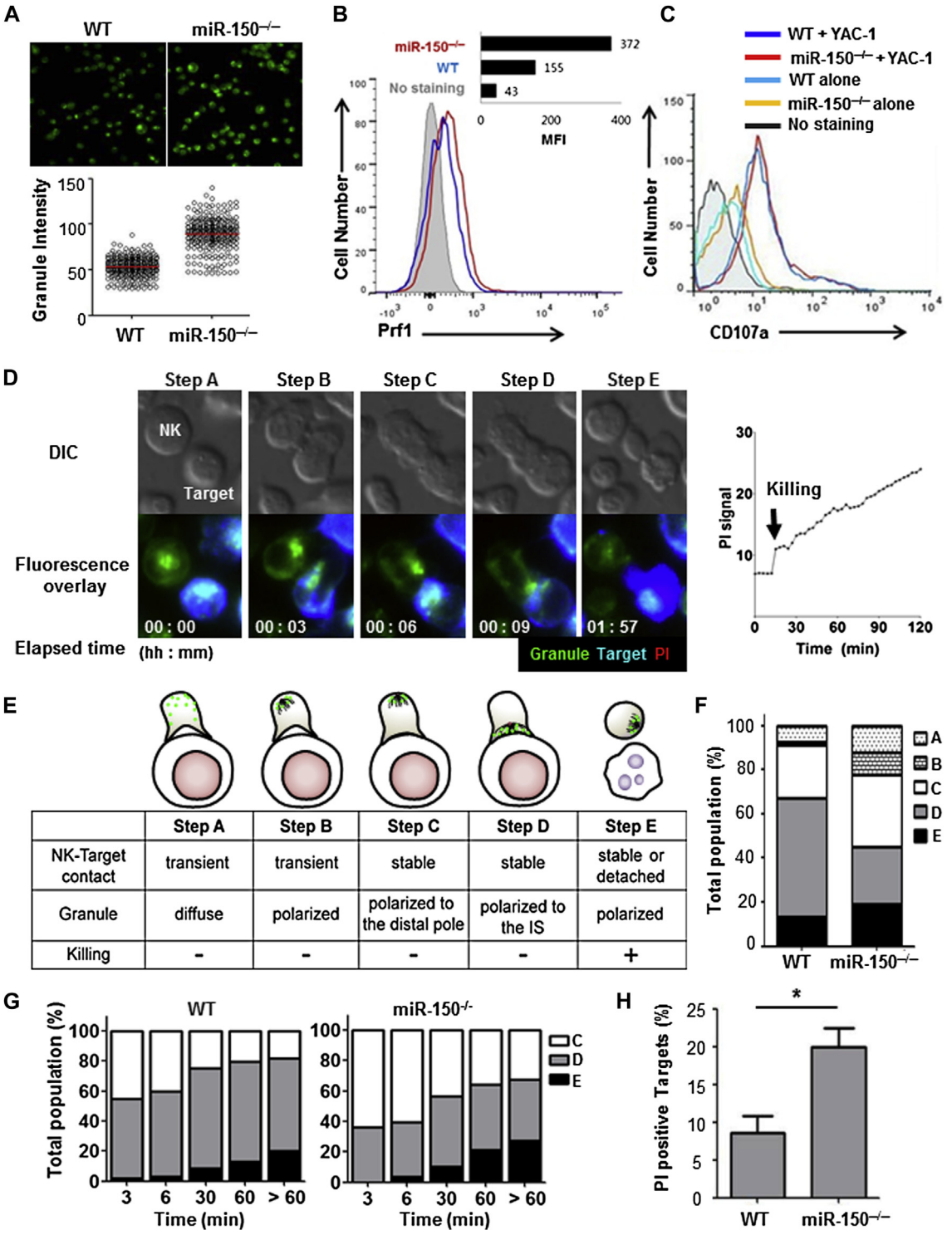

	Step A	Step B	Step C	Step D	Step E
NK-Target contact	transient	transient	stable	stable	stable or detached
Granule	diffuse	polarized	polarized to the distal pole	polarized to the IS	polarized
Killing	-	-	-	-	+

FIG 4. miR-150$^{-/-}$ NK cells induce a potent lytic hit at the immunologic synapse. **A-C,** NK cells were stained with LysoSensor (Fig 4, *A*), Prf1 (Fig 4, *B*), or CD107a (Fig 4, *C*). **D** and **E,** Dynamic interfaces formed between NK cells and target cells were photographed (Fig 4, *D*) and illustrated (Fig 4, *E*). **F-H,** Percentage of NK cells remaining at each step (Fig 4, *F*); kinetics of steps C, D, and E (Fig 4, *G*); and cytotoxicity (Fig 4, *H*). *MFI*, Mean fluorescence intensity. *$P < .05$.

long-term culture with high levels of cytokines have significantly different miRNA expression than freshly isolated primary human NK cells. Liu et al[25] reported that miR-30e repressed Prf1 in human NK cells on IFN-α stimulation. The miR-30e level was shown to be inversely associated with Prf1 protein expression *in vitro*, but its role in immune surveillance against tumor cells *in vivo* remains to be elucidated. Although these studies address the role of miRNAs in human NK cells, extensive research on

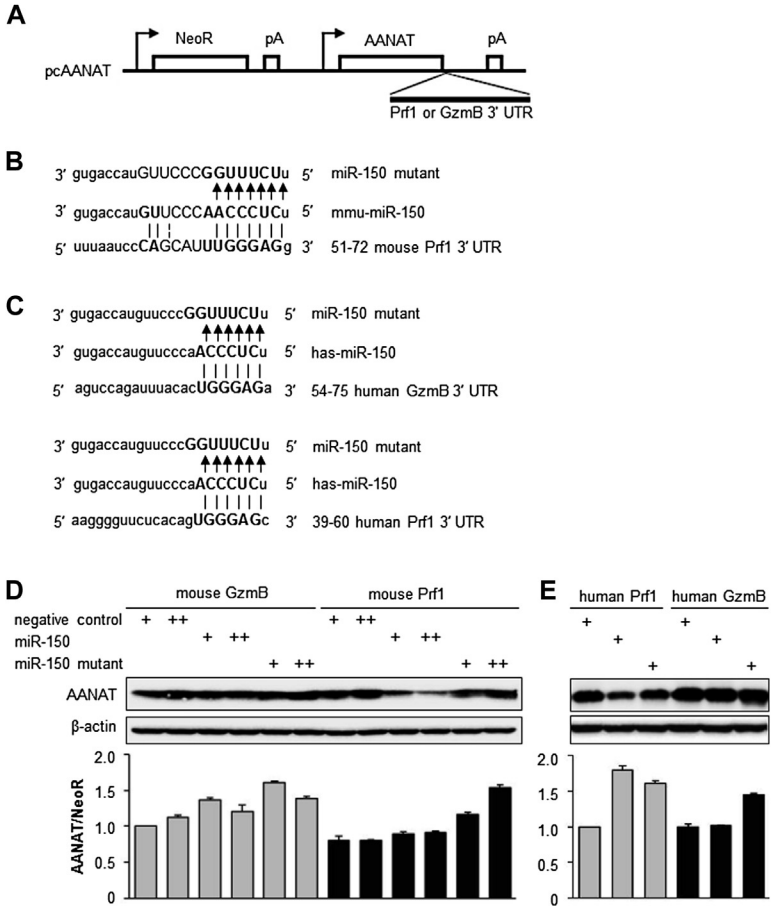

FIG 5. miR-150 directly targets Prf1 in NK cells. **A-C,** Scheme of reporter vector (Fig 5, *A*) and sequence alignments of miR-150 to target cells (Fig 5, *B* and *C*). **D** and **E,** 3′ UTR AANAT reporter containing mouse GzmB/Prf1 (Fig 5, *D*) or human Prf1/GzmB (Fig 5, *E*) were cotransfected with indicated miRNAs, and then AANAT proteins and mRNAs were analyzed. Data represent means ± SDs of 3 independent experiments. +, 50 nmol/L; ++, 100 nmol/L. *pA*, Polyadenylation. $P < .01$.

miRNA-mediated Prf1 regulation in both mouse and human NK cells at rest and at various time points after activation has not been investigated.

Here we report that miR-150 posttranscriptionally regulates Prf1 in freshly isolated primary mouse and human NK cells at rest and after IL-15 activation. Unlike exogenous Prf1 gene transfer to NK cells, which constitutively express Prf1 without stimuli, an inverse correlation between miR-150 levels and Prf1 expression during IL-15 activation serves 2 purposes. First, mature resting or insufficiently activated NK cells contain substantial amounts of endogenous miR-150, which prevents spontaneous activation of the newly generated NK cells without adequate stimuli through repression of pre-existing Prf1 mRNA translation. Second, reduced miR-150 expression in fully activated NK cells allows enhanced production of Prf1 from preformed Prf1 mRNA for prompt and potent immune responses.

Even though miR-150$^{-/-}$ NK cells exhibited amplified Prf1 translation at 48 and 72 hours of IL-15 stimulation, resting miR-150$^{-/-}$ NK cells still minimally express Prf1 protein similarly to resting WT NK cells (Fig 2, *A*, top). Xiao et al[14] also reported that activated miR-150$^{-/-}$ B cells highly expressed c-Myb protein, a known target of miR-150, compared with WT B cells at 48 and 72 hours of anti-IgM stimulation, but resting miR-150$^{-/-}$ B cells minimally expressed c-Myb protein. How resting miR-150$^{-/-}$ NK cells are minimally cytotoxic still needs to be clarified, but this phenomenon makes miR-150$^{-/-}$ NK cells more attractive for adoptive NK cell therapy because of their unique ability to maintain minimal cytotoxicity at rest while exhibiting maximal lytic activity on activation.

miR-150 is highly upregulated in mature B, T, and NK cells but not in their progenitors.[12-16] Ectopic expression of miR-150 in mouse B-cell precursors leads to severe defects in B-cell development at the transition from the pro-B-cell to pre-B-cell stage by targeting c-Myb, but impairment of T-cell development was less severe.[14,26] miR-150$^{-/-}$ mice have significant reductions in NK cell development and maturation.[12] Here we revealed that the same number of miR-150$^{-/-}$ NK cells showed enhanced cytotoxicity compared with that in WT NK cells by augmented Prf1 production, which led to more powerful lytic hits to target cells. Collectively, this implies that miR-150$^{-/-}$ mice might compensate for reduced numbers of mature NK cells by alternately improving NK cell effector function.

miR-150 also plays a critical role as a tumor suppressor by targeting the proto-oncogene c-Myb and Notch3. miR-150 is significantly downregulated in patients with severe sepsis,[27] a

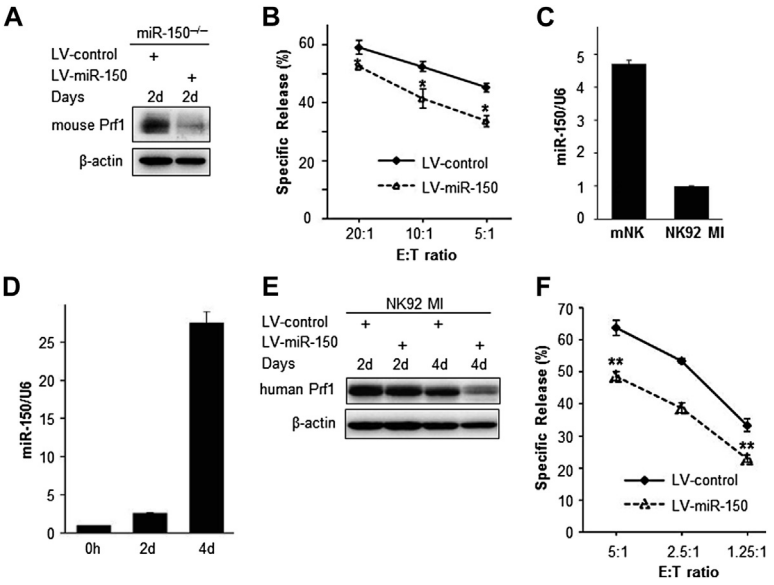

FIG 6. A, B, E, and **F,** Lentivirus *(LV)*–mediated overexpression of miR-150 suppresses Prf1 and cytotoxicity. After lentiviral transduction, miR-150$^{-/-}$ NK and NK92 MI cells showed decreased Prf1 protein (Fig 6, *A* and *E*) and NK cell cytotoxicity (Fig 6, *B* and *F*), respectively. **C** and **D,** Low endogenous miR-150 in NK92 MI cells (Fig 6, *C*) was increased after lentiviral transduction (Fig 6, *D*). Data represent means ± SDs from 3 independent experiments. *mNK,* Mature NK cell. **P* < .05 and ***P* < .01.

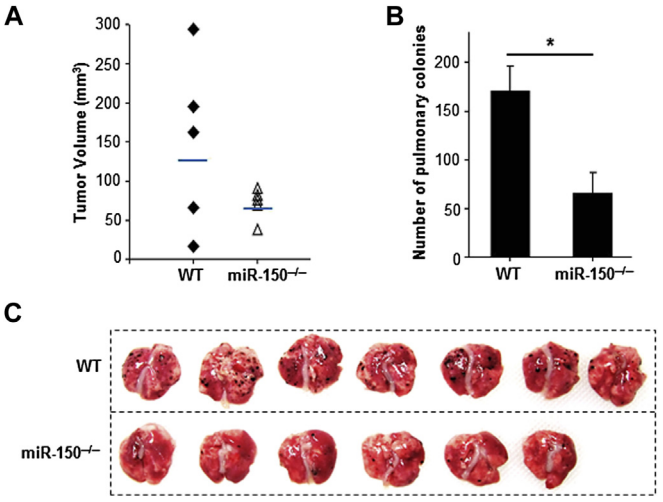

FIG 7. miR-150$^{-/-}$ NK cells exhibit enhanced tumor surveillance in immunocompromised mice. Adoptive transfer of miR-150$^{-/-}$ NK cells effectively reduced tumor growth **(A)** and lung metastasis of B16F10 melanoma **(B** and **C)** compared with that seen in WT NK cells in Rag2$^{-/-}\gamma C^{-/-}$ mice. Data represent means ± SDs of 2 independent experiments. **P* < .05.

broad range of acute leukemias,[28] chronic myeloid leukemias,[29] malignant NK/T-cell lymphomas,[30] colorectal cancers,[31] and hepatocellular carcinomas.[32] Therefore, miR-150 was highly expressed in normal mature NK cells but significantly downregulated in NK92 MI cells derived from a patient with non-Hodgkin lymphoma (Fig 6, *C*). Lentivirus-mediated overexpression of miR-150 in NK/T-cell lymphoma cells resulted in increased expression of tumor suppressors, such as p53 and Bim, and decreased levels of AKT2, becoming more susceptible to the anticancer drug etoposide.[30] On the contrary, the transcription levels of the proto-oncogenes c-Myb, c-kit, and Bcl-2 were increased in sorted miR-150$^{-/-}$ NK cells,[12] which raises the interesting possibility that miR-150$^{-/-}$ NK cells could be more resistant to anticancer drugs.

These data suggest that the downregulation of miR-150 confers a growth advantage to malignant cells, as well as premature and activated lymphocytes, possibly by upregulating c-Myb and Bcl-2. On activation, miR-150 was downregulated in mature B, T, NK, and invariant NK T cells, potentially releasing mature lymphocytes from growth arrest and allowing rapid proliferation to occur for proper immune responses.

In summary, the downregulation of miR-150 can be a promising approach to NK cell therapies by enhancing NK cell cytotoxicity while possibly reducing NK cell apoptosis to anticancer agents. The ultimate goal of immunotherapy in many settings would not only include boosting the tumor-killing ability of immune effector cells but also making the effector cells more resistant to the anticancer drugs being concurrently administered to patients.[33] Additionally, one study reported that allergen-specific cytotoxic T cells require sufficient Prf1 expression to suppress allergic airway inflammation.[34] This implies that NK cells might contribute to Prf1-mediated allergic responses. Actually, NK cells have been reported to be involved in allergic diseases.[35-37] Patients with atopic dermatitis showed defects in NK cell cytotoxicity and IFN-γ production.[38] Thus therapeutic control of miR-150 in NK cells potentially opens new avenues for enhanced miRNA-mediated NK cell immunotherapy against various human pathologies, including cancer and allergy, providing a better clinical outcome.

We thank Youngju Kang, Yeonkyung Kim, Dongo Kim, Sungjin Yoon, Mijeong Kim, Wonsam Kim, Soojin Kim, Sooyoung Jun, and Hyangran Yoon for expert technical assistance. We also thank Haiyoung Jung, Youngjun Park, Sukran Yoon, David Kim, and Gouyoung Koh for fruitful discussions.

Key messages

- **miR-150 posttranscriptionally downregulated Prf1 expression in both mouse and human NK cells at rest and after IL-15 activation.**
- **Activated miR-150$^{-/-}$ NK cells expressed upregulated Prf1, augmenting cytotoxicity.**
- **The adoptive transfer of miR-150$^{-/-}$ NK cells significantly reduced tumor growth and metastasis of B16F10 melanoma in immunocompromised mice.**

REFERENCES

1. Grossman WJ, Revell PA, Lu ZH, Johnson H, Bredemeyer AJ, Ley TJ. The orphan granzymes of humans and mice. Curr Opin Immunol 2003;15:544-52.
2. Henkart PA. Mechanism of lymphocyte-mediated cytotoxicity. Annu Rev Immunol 1985;3:31-58.
3. Russell JH, Ley TJ. Lymphocyte-mediated cytotoxicity. Annu Rev Immunol 2002; 20:323-70.
4. Baran K, Dunstone M, Chia J, Ciccone A, Browne KA, Clarke CJ, et al. The molecular basis for perforin oligomerization and transmembrane pore assembly. Immunity 2009;30:684-95.
5. Voskoboinik I, Thia MC, Fletcher J, Ciccone A, Browne K, Smyth MJ, et al. Calcium-dependent plasma membrane binding and cell lysis by perforin are mediated through its C2 domain: A critical role for aspartate residues 429, 435, 483, and 485 but not 491. J Biol Chem 2005;280:8426-34.
6. Motyka B, Korbutt G, Pinkoski MJ, Heibein JA, Caputo A, Hobman M, et al. Mannose 6-phosphate/insulin-like growth factor II receptor is a death receptor for granzyme B during cytotoxic T cell-induced apoptosis. Cell 2000;103:491-500.
7. Lichtenheld MG, Podack ER. Structure of the human perforin gene. A simple gene organization with interesting potential regulatory sequences. J Immunol 1989;143: 4267-74.
8. Kiessling R, Klein E, Wigzell H. "Natural" killer cells in the mouse. I. Cytotoxic cells with specificity for mouse Moloney leukemia cells. Specificity and distribution according to genotype. Eur J Immunol 1975;5:112-7.
9. Fehniger TA, Cai SF, Cao X, Bredemeyer AJ, Presti RM, French AR, et al. Acquisition of murine NK cell cytotoxicity requires the translation of a pre-existing pool of granzyme B and perforin mRNAs. Immunity 2007;26:798-811.
10. Bartel DP. MicroRNAs: target recognition and regulatory functions. Cell 2009;136: 215-33.
11. Baltimore D, Boldin MP, O'Connell RM, Rao DS, Taganov KD. MicroRNAs: new regulators of immune cell development and function. Nat Immunol 2008;9:839-45.
12. Bezman NA, Chakraborty T, Bender T, Lanier LL. miR-150 regulates the development of NK and iNKT cells. J Exp Med 2011;208:2717-31.
13. Fedeli M, Napolitano A, Wong MP, Marcais A, de Lalla C, Colucci F, et al. Dicer-dependent microRNA pathway controls invariant NKT cell development. J Immunol 2009;183:2506-12.
14. Xiao C, Calado DP, Galler G, Thai TH, Patterson HC, Wang J, et al. MiR-150 controls B cell differentiation by targeting the transcription factor c-Myb. Cell 2007; 131:146-59.
15. Zheng Q, Zhou L, Mi QS. MicroRNA miR-150 is involved in Valpha14 invariant NKT cell development and function. J Immunol 2012;188:2118-26.
16. Zhou B, Wang S, Mayr C, Bartel DP, Lodish HF. miR-150, a microRNA expressed in mature B and T cells, blocks early B cell development when expressed prematurely. Proc Natl Acad Sci U S A 2007;104:7080-5.
17. Oshimi Y, Oda S, Honda Y, Nagata S, Miyazaki S. Involvement of Fas ligand and Fas-mediated pathway in the cytotoxicity of human natural killer cells. J Immunol 1996;157:2909-15.
18. Vanherberghen B, Olofsson PE, Forslund E, Sternberg-Simon M, Khorshidi MA, Pacouret S, et al. Classification of human natural killer cells based on migration behavior and cytotoxic response. Blood 2013;121:1326-34.
19. Peters PJ, Borst J, Oorschot V, Fukuda M, Krahenbuhl O, Tschopp J, et al. Cytotoxic T lymphocyte granules are secretory lysosomes, containing both perforin and granzymes. J Exp Med 1991;173:1099-109.
20. Kim TD, Lee SU, Yun S, Sun HN, Lee SH, Kim JW, et al. Human microRNA-27a* targets Prf1 and GzmB expression to regulate NK-cell cytotoxicity. Blood 2011; 118:5476-86.
21. Colucci F, Soudais C, Rosmaraki E, Vanes L, Tybulewicz VL, Di Santo JP. Dissecting NK cell development using a novel alymphoid mouse model: investigating the role of the c-abl proto-oncogene in murine NK cell differentiation. J Immunol 1999;162:2761-5.
22. Smyth MJ, Thia KY, Cretney E, Kelly JM, Snook MB, Forbes CA, et al. Perforin is a major contributor to NK cell control of tumor metastasis. J Immunol 1999;162: 6658-62.
23. Sullivan RP, Leong JW, Fehniger TA. MicroRNA regulation of natural killer cells. Front Immunol 2013;4:44.
24. Leong JW, Sullivan RP, Fehniger TA. Natural killer cell regulation by microRNAs in health and disease. J Biomed Biotechnol 2012;2012:632329.
25. Liu X, Wang Y, Sun Q, Yan J, Huang J, Zhu S, et al. Identification of microRNA transcriptome involved in human natural killer cell activation. Immunol Lett 2012; 143:208-17.
26. Lu J, Guo S, Ebert BL, Zhang H, Peng X, Bosco J, et al. MicroRNA-mediated control of cell fate in megakaryocyte-erythrocyte progenitors. Dev Cell 2008;14: 843-53.
27. Vasilescu C, Rossi S, Shimizu M, Tudor S, Veronese A, Ferracin M, et al. MicroRNA fingerprints identify miR-150 as a plasma prognostic marker in patients with sepsis. PLoS One 2009;4:e7405.
28. Jiang X, Huang H, Li Z, Li Y, Wang X, Gurbuxani S, et al. Blockade of miR-150 maturation by MLL-fusion/MYC/LIN-28 is required for MLL-associated leukemia. Cancer Cell 2012;22:524-35.
29. Agirre X, Jimenez-Velasco A, San Jose-Eneriz E, Garate L, Bandres E, Cordeu L, et al. Down-regulation of hsa-miR-10a in chronic myeloid leukemia CD34+ cells increases USF2-mediated cell growth. Mol Cancer Res 2008; 6:1830-40.
30. Watanabe A, Tagawa H, Yamashita J, Teshima K, Nara M, Iwamoto K, et al. The role of microRNA-150 as a tumor suppressor in malignant lymphoma. Leukemia 2011;25:1324-34.
31. Ma Y, Zhang P, Wang F, Zhang H, Yang J, Peng J, et al. miR-150 as a potential biomarker associated with prognosis and therapeutic outcome in colorectal cancer. Gut 2012;61:1447-53.
32. Jiang J, Gusev Y, Aderca I, Mettler TA, Nagorney DM, Brackett DJ, et al. Association of MicroRNA expression in hepatocellular carcinomas with hepatitis infection, cirrhosis, and patient survival. Clin Cancer Res 2008;14:419-27.
33. Markasz L, Stuber G, Vanherberghen B, Flaberg E, Olah E, Carbone E, et al. Effect of frequently used chemotherapeutic drugs on the cytotoxic activity of human natural killer cells. Mol Cancer Ther 2007;6:644-54.
34. Enomoto N, Hyde E, Ma JZ, Yang J, Forbes-Blom E, Delahunt B, et al. Allergen-specific CTL require perforin expression to suppress allergic airway inflammation. J Immunol 2012;188:1734-41.
35. Wei H, Zhang J, Xiao W, Feng J, Sun R, Tian Z. Involvement of human natural killer cells in asthma pathogenesis: natural killer 2 cells in type 2 cytokine predominance. J Allergy Clin Immunol 2005;115:841-7.
36. Farhadi N, Lambert L, Triulzi C, Openshaw PJ, Guerra N, Culley FJ. Natural killer cell NKG2D and granzyme B are critical for allergic pulmonary inflammation. J Allergy Clin Immunol 2013 [Epub ahead of print].
37. Deniz G, van de Veen W, Akdis M. Natural killer cells in patients with allergic diseases. J Allergy Clin Immunol 2013;132:527-35.
38. Luci C, Gaudy-Marqueste C, Rouzaire P, Audonnet S, Cognet C, Hennino A, et al. Peripheral natural killer cells exhibit qualitative and quantitative changes in patients with psoriasis and atopic dermatitis. Br J Dermatol 2012;166: 789-96.

METHODS

Mice

WT C57BL/6J, miR-150$^{-/-}$, and Rag2$^{-/-}\gamma C^{-/-}$ mice were purchased from Jackson Laboratories and were bred and maintained under specific pathogen-free conditions. For mouse experiments, sex- and age-matched 8- to 12-week-old mice were used in accordance with the guidelines of the KRIBB Institutional Animal Care and Use Committee. The KRIBB Animal Welfare Assurance number was KRIBB-AEC-11039.

Primary NK cell preparations and cell culture

Primary mouse NK cells were isolated from the spleen by using the mouse NK Cell Isolation Kit II (Miltenyi Biotec, Bergisch Gladbach, Germany), according to the manufacturer's protocol. Enriched mouse NK cells (>90% NK1.1$^+$) were cultured in RPMI 1640 (WelGENE, Daegu, Korea) containing 10% FBS (Thermo Scientific Hyclone) and 1% penicillin-streptomycin-amphotericin B (WelGENE) supplemented with either 25 or 100 ng/mL recombinant mouse IL-15 (PeproTech, Rocky Hill, NJ), depending on the purpose of the experiments. Primary human NK cells were obtained from umbilical cord blood by using ACCUSPIN System-Histopaque-1077 (Sigma-Aldrich, St Louis, Mo) density separation. NK cells were then enriched by means of negative selection with the MACS NK cell isolation kit, according to the manufacturer's instructions (Miltenyi Biotec). Highly enriched NK cell populations (>93% CD56$^+$/CD3$^-$ and <5% CD3$^+$) were maintained in IL-15 (30 ng/mL)–supplemented culture medium. Human CD34$^+$ hematopoietic precursors were differentiated *in vitro* from umbilical cord blood, as described previously,[E1] to obtain *in vitro*–differentiated human NK cells. The populations of terminally differentiated mature NK cells were 90% CD56$^+$CD3$^-$ or greater. The YAC-1 and K562 cells were cultured in RPMI 1640 (WelGENE) supplemented with 10% FBS (Hyclone) and 1% penicillin-streptomycin-amphotericin B (WelGENE; referred to as complete RPMI medium). The human NK cell line NK92 MI was cultured in α-MEM (Gibco, Carlsbad, Calif) supplemented with 20% heat-inactivated FBS (Hyclone) and 2 mmol/L L-glutamine. Human embryonic kidney (HEK) 293FT cells and B16/F10 cells were maintained in Dulbecco modified Eagle medium (DMEM) containing 10% FBS and 1% penicillin-streptomycin-amphotericin B (referred to as complete DMEM medium). Cells were maintained under 37°C and 5% CO_2 conditions.

Lentiviral transduction

For lentiviral transduction, the pMIRNA1-GFP control vector and pMIR-150 vector encoding precursor-miR-150 were obtained from System Biosciences (Mountain View, Calif). Lentiviruses were produced by using a third-generation packaging system (pMDLg/pRRE, pRSV-Rev, and pMD2.G) in HEK293FT cells, as previously described,[E2] with minor modifications. After 48 hours of transfection, the lentivirus-containing supernatants were filtered through a 0.45-μm filter and mixed with PEG-it Virus Precipitation Solution (System Biosciences) overnight, concentrated by means of centrifugation at 1500*g* for 30 minutes at 4°C, and stored at −70°C. Frozen infectious supernatants were used to infect primary mouse NK cells or human NK92 MI cells. Transduced cells were replenished with half the amount of fresh medium every 24 hours and allowed to grow for approximately 48 to 96 hours, depending on the cell types.

Kinetic analysis of effector molecule expression

Primary human and mouse NK cells were freshly incubated in the presence of IL-15 (30 ng/mL). The cells were harvested at the times indicated (0, 6, 12, 24, and 48 or 72 hours) relative to IL-15 addition. Kinetic analysis of Prf1 and GzmB expression in NK cells during activation was performed with immunoblot analyses and cDNA quantification by means of semiquantitative PCR or real-time quantitative PCR analyses by using the specific primer pairs shown in Table E1. Band intensities of Prf1 and GzmB proteins and cDNAs were normalized with those of glyceraldehyde-3-phosphate dehydrogenase (GAPDH) or actin and plotted as a relative amount at time zero (0 hours, value 1). The quantitative data are expressed as the mean value of independent measurements from 2 separate experiments (mean ± SEM).

In vivo tumor challenge experiments

Purified mouse NK cells (6×10^5) were cultured in a high concentration of mouse IL-15 (100 ng/mL) for 24 hours and then injected intravenously into Rag2$^{-/-}\gamma C^{-/-}$ recipient mice (n = 5). After 2 hours, B16F10 cells (4×10^5) were injected subcutaneously into the shaved lateral flanks of those mice. The size of primary tumors was monitored on day 11 with a caliper. Tumor volume was calculated with the following formula:

$$V = (A \times B \times C)/2,$$

where V is defined as volume (in cubic millimeters), A if defined as length (in millimeters), B is defined as width (in millimeters), and C is defined as height (in millimeters). A well-established experimental lung metastasis model was used with modifications to validate NK cell–mediated control of lung metastasis.[E3] WT and miR-150$^{-/-}$ NK cells (2×10^5 cells) were stimulated with high-dose IL-15 (100 ng/mL) for 12 hours and injected intravenously into Rag2$^{-/-}\gamma C^{-/-}$ mice. B16F10 melanoma cells (1×10^5 cells) were injected into the tail veins of Rag2$^{-/-}\gamma C^{-/-}$ mice 2 days after NK cell injection. Lungs were harvested and examined visually for melanoma clones after 14 days. Numbers of pulmonary metastatic colonies were quantitated by means of counting.

Semiquantitative PCR and real-time PCR

Total RNAs were extracted from cells by using an RNA-spin kit (iNtRON Biotechnology, Gyeonggi-do, South Korea), and 1 μg of RNA was reverse transcribed into cDNA by using a ReverTra Ace α–First Strand cDNA Synthesis Kit (Toyobo, Osaka, Japan), according to the manufacturer's protocol. For semiquantitative PCR, 27 cycles of PCR amplification were performed as follows: 95°C for 30 seconds, 55°C for 30 seconds, and 72°C for 30 seconds, followed by an extension step at 72°C for 5 minutes. The PCR products were visualized with agarose gel electrophoresis and ethidium bromide. Real-time PCR was performed with a Dice TP800 Thermal Cycler (Takara Bio, Shiga, Japan) and the SYBR Premix Ex Tag (Takara Bio). The data were normalized to the amount of GAPDH transcript. The primer sequences are shown in Table E1. For real-time PCR of mature miR-150, total RNAs were extracted with an RNeasy mini kit (Qiagen, Hilden, Germany) and reverse transcribed with the TaqMan MicroRNA Reverse Transcription Kit. The level of miR-150 was examined by using the TaqMan MicroRNA Assays specific for miR-150 (Applied Biosystems, Foster City, Calif), and U6 small nuclear RNA was used to normalize the relative abundance of miR-150, according to the manufacturer's instructions.

Western blotting

Cells were washed with PBS and lysed in RIPA buffer (Thermo Fisher Scientific, Waltham, Mass) supplemented with a protease inhibitor cocktail set III (Calbiochem, San Diego, Calif). After rapid sonication, the cell lysates were electrophoresed on 10% Tris-glycine SDS-polyacrylamide gels and transferred to a polyvinylidene difluoride membrane (Millipore, Temecula, Calif). The membranes were incubated with anti-mouse Prf1 (Cell Signaling, Danvers, Mass), anti-GzmB (Abcam, Cambridge, United Kingdom), anti-human Prf1 (Abcam), anti-AANAT (gift from Dr Klein), and anti–β-actin (Sigma-Aldrich), followed by anti-rabbit or anti-mouse IgG (Jackson ImmunoResearch, West Grove, Pa) conjugated to horseradish peroxidase. Immunoreactive bands were visualized with SuperSignal West Pico Chemiluminescent Substrate (Pierce, Rockford, Ill) or Immobilon Western Chemiluminescent HRP Substrate (Millipore) and photographed with EZ-capture (ATTO, Amherst, NY).

NK cell cytotoxicity assays

NK cell–mediated cytotoxicity was examined with a standard 4-hour ^{51}Cr-release assay or calcein-AM cytotoxicity assay. In brief, YAC-1 cells were incubated with 1.5 μCi of ^{51}Cr, and K562 cells were incubated with 15 μmol/L calcein-AM for 1 hour. The ^{51}Cr-labeled YAC-1 cells or calcein-AM–labeled K562 cells (1×10^4 cells per well) were placed into a 96-well round-bottom plate in triplicate and cocultured either with mouse or human NK cells at E/T ratios ranging from 20:1 to 1.25:1 for 4 hours. The ^{51}Cr release

from lysed YAC-1 cells by mouse NK cells was quantified by using a γ-counter, and the calcein release from lysed K562 cells by human NK cells was measured with a spectrofluorometer (excitation filter, 485 nm; emission filter, 535 nm). The percentage of specific lysis was calculated according to the following formula:

$$(\text{Experimental release} - \text{Spontaneous release})/(\text{Maximum release} - \text{Spontaneous release}) \times 100.$$

Spontaneous release refers to ^{51}Cr or calcein released from target cells in complete medium alone, whereas maximum release refers to ^{51}Cr or calcein released from target cells in complete medium containing 1% Triton X-100. To investigate the effect of activating receptors on NK cell cytotoxicity between WT and miR-150$^{-/-}$ NK cells, we pretreated IL-15–activated primary mouse NK cells with 5 μg/mL anti-NKp46 antibody (BioLegend, San Diego, Calif) for 2 hours before the cytotoxicity assay. Next, we stained NK cells alone with phycoerythrin-conjugated anti-mouse CD107a (BD Biosciences, San Jose, Calif) or NK cells cocultured with YAC-1 target cells (1×10^4) for 2 hours at 37°C and performed by using standard flow cytometry.

Flow cytometry

Purified mouse NK cells were cultured in complete RPMI medium supplemented with IL-15 (25 ng/mL) for 48 hours. Activated NK cells (1×10^5) were resuspended in PBS containing 1% FBS and stained for 20 minutes at 4°C with 1 or 2 of the following antibodies: phycoerythrin-conjugated anti-mouse-NKG2D, CD122, CD132, CD95, CXCR5, CCR6, or Ly49C/I or fluorescein isothiocyanate–conjugated anti-mouse-NKp46, Ly49D, Ly49A, or Ly49G2 (from BD Biosciences, BioLegend, or eBioscience). For the degranulation assay, IL-15–activated NK cells (1×10^5) were stained with phycoerythrin-conjugated anti-mouse CD107a (BD Biosciences) and either used alone or cocultured with YAC-1 target cells (1×10^4) for 1 hour at 37°C in the dark, and unstained NK cells alone served as a negative control. Golgi-stop (BD Biosciences) was added at a final concentration of 6 μg/mL and incubated for an additional 4 hours at 37°C. For the detection of intracytoplasmic Prf1 in NK cells, mixed cell populations were stained with allophycocyanin-conjugated anti-mouse NK1.1 (BD Biosciences) for 30 minutes at 4°C, fixated, and then permeabilized for 20 minutes at 4°C. After staining with anti-mouse Prf1 antibody, flow cytometry was performed on a BD FACSCanto II device, and data were analyzed with FlowJo software (Tree Star).

Live cell imaging

NK cells (1×10^7/mL) were loaded with 1 μg/mL of LysoSensor Green DND-153 (Invitrogen, Carlsbad, Calif) by incubating at 37°C for 30 minutes. YAC-1 cells (5×10^6/mL) were labeled with 10 μg/mL CellTrace Far Red DDAO-SE (Invitrogen) by incubating at 37°C for 15 minutes. The LysoSensor-labeled NK cells (approximately 2-5 $\times 10^5$) in complete RPMI medium containing 10 μg/mL PI were seeded onto an anti-CD44–coated glass cover slip loaded in a Chamlide magnetic chamber (Live Cell Instrument, Seoul, Korea). The NK cell–seeded chamber was mounted on a microscope stage equipped with a Chamlide TC incubator system (Live Cell Instrument), maintained at 37°C and 5% CO_2, and incubated for 30 minutes. Then DDAO-labeled YAC-1 target cells were gently added into the magnetic chamber containing NK cells, and time-lapse imaging was performed in 3-minute intervals for 2 hours. A modified Zeiss Axio Observer Z1 epi-fluorescence microscope (Zeiss, Oberkochen, Germany) with a 40X (Plan-Neofluar, NA = 1.30) objective lens and a Roper Scientific CoolSnap HQ CCD camera (Roper Scientific, Ottobrunn, Germany) were used for imaging. Differential Interference Contrast (DIC) and green (LysoSensor, EX BP 470/40, BS 495, EMBP 525/50), red (PI, EX BP 550/25, BS 570, EMBP 605/70), and far red (DDAO, EX BP 620/60, BS 660, EMBP 770/75) fluorescence images were acquired in rapid succession at each time interval. For LysoSensor imaging, 3 optical section images over 1.5-μm distances in the z-direction were acquired and integrated. Image processing and analysis were performed with ImageJ software (National Institutes of Health) and Metamorph (Molecular Devices, Sunnyvale, Calif).

Plasmid constructions

Total RNAs were extracted from mouse primary NK cells or human NK92 cells and reverse transcribed with oligo(dT) to construct chimeric AANAT reporter plasmids (Toyobo). The cDNAs for human and mouse Prf1 and GzmB 3′ UTRs were amplified with specific primers (Table E2), and the amplification of cDNA was confirmed by means of sequencing. The PCR products of human Prf1, human GzmB, and mouse Prf1 were digested with *EcoR*I and *Xba*I, and the PCR product of mouse GzmB was cleaved with *Xho*I and then cloned into the *EcoRI*/*Xba*I sites and the blunt/*XhoI* site of the reporter pcAANAT,[E4] respectively.

Transfection

For AANAT reporter assays, HEK293FT cells were seeded at 4×10^5 cells per well in 12-well plates without antibiotics and grown overnight. After the cells reached 85% to 90% confluence, they were cotransfected with 1 μg of AANAT plasmids containing 3′ UTR of Prf1 or GzmB combined with either miR-150 mimics, miR-150 mutants, or a nontargeting control (Dharmacon, Lafayette, Colo) at concentrations of approximately 50 to 100 nmol/L by using Lipofectamine 2000 and Plus (Invitrogen), per the manufacturer's protocol. After 16 hours of transfection, transfection medium was replaced with complete DMEM medium, and cells were grown for a further 48 hours.

Statistical analyses

Comparisons between samples were analyzed for statistical significance by using the Student *t* test with Microsoft Excel software. A *P* value of less than .05 was considered significant.

REFERENCES

E1. Lee SH, Yun S, Lee J, Kim MJ, Piao ZH, Jeong M, et al. RasGRP1 is required for human NK cell function. J Immunol 2009;183:7931-8.

E2. Dull T, Zufferey R, Kelly M, Mandel RJ, Nguyen M, Trono D, et al. A third-generation lentivirus vector with a conditional packaging system. J Virol 1998; 72:8463-71.

E3. Andrews DM, Sullivan LC, Baschuk N, Chan CJ, Berry R, Cotterell CL, et al. Recognition of the nonclassical MHC class I molecule H2-M3 by the receptor Ly49A regulates the licensing and activation of NK cells. Nat Immunol 2012; 13:1171-7.

E4. Kim TD, Kim JS, Kim JH, Myung J, Chae HD, Woo KC, et al. Rhythmic serotonin N-acetyltransferase mRNA degradation is essential for the maintenance of its circadian oscillation. Mol Cell Biol 2005;25:3232-46.

TABLE E1. Primer sequences used for real-time PCR

Gene name	Direction	Sequence
Human Prf1	Forward	5′-GCTGGACGTGACTCCTAAGC-3′
	Reverse	5′-GATGAAGTGGGTGCCGTAGT-3′
Human GzmB	Forward	5′-GTAAGGGGGAAACAACAGCA-3′
	Reverse	5′-CCCCAAGGTGACATTTATGG-3′
Mouse Prf1	Forward	5′-TTCGGGAACCAAGCTACACCA-3′
	Reverse	5′-CAGGCTGTAGTCCACCAGACCA-3′
Mouse GzmB	Forward	5′-AAGAACTGGGTGTTGACTGCTG-3′
	Reverse	5′-CACGTGTATATTCATCATAGCATGG-3′
NeoR	Forward	5′-ATGACTGGGCACA-ACAGACA-3′
	Reverse	5′-AGTGACAACGTCGAGCACAG-3′
AANAT	Forward	5′-CATCTGCCTCTTGGGACCT-3′
	Reverse	5′-AGCTCTGGACACAGGGTGAG-3′
Mouse GAPDH	Forward	5′-TCAACAGCAACTCCCACTCTTCCA-3′
	Reverse	5′-ACCCTGTTGCTGTAGCCGTA-TTCA-3′
Human GAPDH	Forward	5′-GCCATCAATGACCCCTTCATT-3′
	Reverse	5′-GCTCCTGGAAGATGGTGGTGATGG-3′

TABLE E2. Oligonucleotides used to generate AANAT reporter plasmids containing the 3′ UTR of Prf1 or GzmB in mice or human subjects

Inserts	Direction	Sequence
Mouse Prf1 3′ UTR	Forward	5′-AAGAATTCTAACATAATAACA-3′
	Reverse	5′-AATCTAGAGGGAGAAGGGATTTAAAG -3′
Mouse GzmB 3′ UTR	Forward	5′-AAGAATTCTACAGAAGCAACATGGA-3′
	Reverse	5′-AACTCGAGATCAGGTTATACCTTGA -3′
Human Prf1 3′ UTR	Forward	5′-AAGAATTCTGAGAACAGTGAGCTTGG-3′
	Reverse	5′-AATCTAGACACCATAACATCATATT -3′
Human GzmB 3′ UTR	Forward	5′-AAGAATTCCTACAGGA-AGCAAACTA -3′
	Reverse	5′-AATCTAGACCACTCAGCTAAGAGGT-3′

Flanking sequences for cloning purposes are underlined.